JMEPEG (2012) 21:1479–1484
DOI: 10.1007/s11665-011-0040-z

1059-9495/$19.00

Effects of Pre-Strain on Exfoliation Corrosion Behavior in Al-Cu-Mg Alloy

Yao Li, Zhiyi Liu, Song Bai, Lianghua Lin, and Lifang Gao

(Submitted May 29, 2011; in revised form July 15, 2011)

Mechanical properties and exfoliation corrosion behavior in Al-Cu-Mg alloy with various pre-strain percents were characterized in this study by means of hardness measurement, optical microscope, transmission electron microscope (TEM), x-ray diffraction (XRD), and electrochemical technique. The hardness of naturally aged alloy was significantly enhanced with increasing the pre-strain percents. The immersion tests and polarization measurements revealed that the pre-straining processing before natural aging reduced the resistance of the alloy to exfoliation corrosion (EXCO), which was mainly attributed to the increase of dislocations density and grain aspect ratio. The decrease of residual tensile stress may only play a minor role in the EXCO resistance.

Keywords Al-Cu-Mg alloy, dislocations density, exfoliation corrosion, grain shape, pre-strain, residual stress

1. Introduction

The 2000 series alloys are widely used in the aircraft industry-related fields because of their high strength-to-weight ratio, superior high-temperature properties, resistance-to-fatigue crack propagation, and fracture toughness (Ref 1-3). For Al-Cu-Mg alloys in the (α + S) phase field, the precipitation hardening and precipitates have been extensively studied (Ref 4-6). The precipitation sequence of the alloy can be expressed as SSS $\rightarrow$ GPB $\rightarrow$ S″ $\rightarrow$ S′ $\rightarrow$ S (Ref 5), where GPB is the Cu/Mg Guinier-Preston-Bagariastkij zones, S″ and S′ are the metastable Al_2CuMg phases, and S is the equilibrium Al_2CuMg.

Exfoliation is a localized kind of corrosion that occurs on the surface of high-strength wrought aluminum alloys with an elongated grain structure. Previous studies have suggested that the grain shape and heat treatment conditions have significant effects on the exfoliation corrosion of the alloy (Ref 7, 8). Based on the research by Robinson and Jackson (Ref 7), the exfoliation corrosion resistances of 2014 and 2024 alloys strongly depended on the grain aspect ratio of the material, with the most sever exfoliation occurring on the mid-section of the plane, which is attributed to the more elongated shape of the grains in this plane. Overaging the alloy is beneficial in lowering the susceptibility to exfoliation corrosion by reducing the rate of intergranular corrosion (IGC) (Ref 8). The exfoliation corrosion is a form of IGC in nature and requires a tensile component of stress at the developing corrosion tip. Liu et al. (Ref 9, 10) investigated the effects of stress on IGC of AA2024-T3, and revealed that the applied compressive stress at a level halfway to yield stress significantly reduced the growth kinetics of IGC in the perpendicular direction, whereas the tensile stress accelerated the corrosion rate of the alloy.

A pre-straining processing before aging is usually applied to aluminum alloys in the as-quenched state to achieve the straightening of products, relive quench-induced internal stress, and improve the mechanical properties (Ref 11, 12). The formation of dislocations that generated in this process greatly influences the subsequent precipitation process and final mechanical response of the alloy. Al-Cu-Mg alloy is generally used as T3 temper, which involved that the alloy was solution treated, then immediately cold worked, and finally naturally aged for at least 100 h. A pre-strain applied to 2024-T3 alloy raised the strength of the alloy, while the growth rate of fatigue crack was increased because of the smaller plastic zone size and less crack closures in the pre-strained material (Ref 13).

Although EXCO behavior and the influence of pre-stain on mechanical properties of 2000 series alloys are well documented (Ref 7-10, 13), studies of the effect of pre-strain before natural aging on EXCO behavior of Al-Cu-Mg alloys are limited. Therefore, the purpose of this study was to investigate the EXCO behavior of naturally aged Al-Cu-Mg alloy with various pre-strain percents. In addition, the effects of the change in dislocations density, grain aspect ratio, and residual stress of the alloy on the exfoliation corrosion have been analyzed and discussed in detail.

2. Experimental Procedure

The chemical composition of experimental alloy used in the present study was Al-3.78Cu-1.67Mg-0.67Mn-0.13Zr (wt.%). The ingot was homogenized at 490 °C for 24 h, and then hot rolled to thin sheet approximately 2 mm in thickness. Strips of

Yao Li, Zhiyi Liu, Song Bai, Lianghua Lin, and **Lifang Gao**, Key Laboratory of Nonferrous Metal Materials Science and Engineering, Ministry of Education, Central South University, Changsha 410083, China; and School of Materials Science and Engineering, Central South University, Changsha 410083, China. Contact e-mail: liuzhiyi@mail.csu.edu.cn.

material were solution treated at 505 °C for 1 h in an air-circulating furnace followed by quenching in water at room temperature (RT). Pre-straining was immediately performed after quenching along the rolling direction under the permanent elongation of 0-10%. Then, all the samples were naturally aged at RT for more than 100 h.

The accelerated EXCO test was performed at RT conforming to EXCO test of ASTM G34-01 standard (Ref 14). Specimens with 100 × 30 mm were prepared from the rectangular cold-rolled sheet in which the long axis of the rectangle was parallel to rolled-direction. The EXCO solution consisted of 234 g NaCl, 50 g KNO_3, and 6.3 mL HNO_3 (65%) diluted to 1 dm^3 solution with deionized water, and the composition of EXCO solution is 4.0 M NaCl + 0.5 M KNO_3 + 0.1 M HNO_3, which has an apparent pH of 0.4. The electrolyte volume-electrode surface area ratio was 15 mL cm^{-2}. Potentiodynamic polarization curves were carried out on a Solartron 1287 electrochemical system with a scan rate of 2 mV s^{-1}. The test solution was the same as the EXCO solution.

Hardness measurement was conducted on a HV-10B Vickers Hardness tester with a load of 3 kg. Metallographic microstructure analyses were performed on a POLYVER-MET metallographic microscope. A Rigaku D/Max 2500 pc x-ray diffractometer with Cu anode was employed to measure the residual stress of the samples. Specimens for TEM were punched mechanically for thin slices of 3 mm in diameter and twin-jet electrolytically polished with a voltage of 10-15 V in a solution of 70% methanol and 30% nitric acid at approximately −20 °C. The TEM observations were examined on a TECNAI G^2 20 transmission electron microscope operating at 200 kV.

3. Results

3.1 Hardness Tests

The hardness curve of Al-3.78Cu-1.67Mg alloy for different pre-strain conditions is shown in Fig. 1. It can be seen that the hardness of the alloy was significantly improved with increasing the pre-strain percents. The hardness of the nonstretched alloy was 127 HV, whereas that of 10% pre-strained alloy was enhanced by 12%. The result of hardness test was consistent with the Ref 15, because of an increase in the density of dislocations.

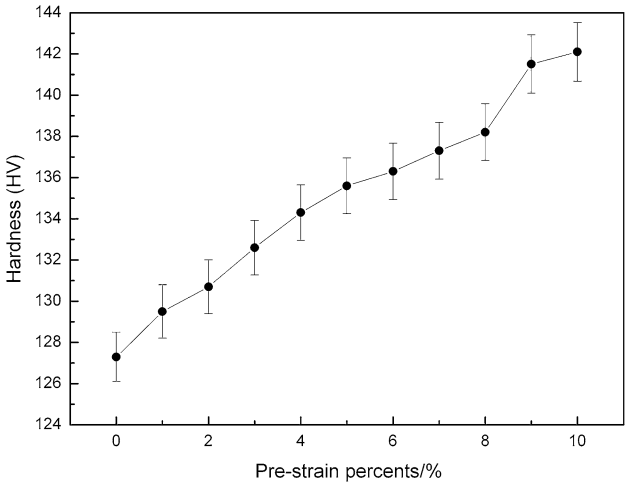

Fig. 1 Hardness curve of Al-3.78Cu-1.67Mg alloy for different pre-strain conditions

3.2 Exfoliation Tests

Figure 2 presents photographs of 0 and 10% pre-strained samples after various times of exfoliation test. According to ASTM G34-01 standard (Ref 14), the visual ratings recorded in the EXCO test are summarized in Table 1. The surface appearances of 0% pre-strained sample did not obviously change until it was exposed for 48 h in the test solution. When exposed for 48-96 h, only the number of pitting increased, and the corrosion pattern on the surface of sample changed from the P^- (superficial pitting) to the P^+ (severe pitting) state. While for 10% pre-strained sample, superficial pitting was observed when it is exposed for 24 h in the EXCO solution. When exposed for 96 h, large pits and powdering exist on the surface, and the alloy was ranked as EA (superficial exfoliation). On comparing with both the samples, it was obvious that the 10% pre-strained sample was more sensitive to EXCO than the 0% pre-strained sample. This indicated that the pre-staining processing before natural aging improved the EXCO susceptibility of Al-3.78Cu-1.67Mg alloy.

3.3 Polarization Measurements

In order to further understand the effect of pre-strain on exfoliation corrosion behavior of the alloy, anodic polarization curves of the samples with a pre-strain of 0 and 10% were performed, as shown in Fig. 3. Tafel extrapolation method based on electrochemical polarization was employed to measure the corrosion potential (E_{corr}) and the corrosion current density (I_{corr}). Electrochemical characteristics derived from the polarization curves are summarized in Table 2. The E_{corr} shifted from −479.1 mV in 0% pre-strained sample to −425.6 mV in 10% pre-strained sample, and the I_{corr} increased from 5.04 to 10.3 μA cm^{-2} correspondingly. According to Faraday's law, the electrochemical corrosion rate (K) can be expressed as

$$K = \frac{3600 A I_{corr}}{nF} \quad \text{(Eq 1)}$$

where A is the relative atomic mass, n is the number of valence of the metal, and F is Faraday constant. It can be seen from Eq 1 that the electrochemical corrosion rate, K, increases linearly with the corrosion current density I_{corr}. The 10% pre-strained sample had higher corrosion current density, and it is thus logical to assume that pre-straining processing decreased the resistance of the alloy to exfoliation corrosion, which was in accordance with the observations of the surface rating.

3.4 Microstructural Characterization

Figure 4 illustrates the optical micrographs of cross section for the samples with a pre-strain of 0 and 10%. Recrystallization occurred completely in both the samples, whereas the grains of the 10% pre-strained specimen were elongated to some extent in contrast to non-deformed specimen. It was suggested that the pre-straining processing increased the grain aspect ratio of the alloy.

Figure 5 is the TEM bright field images and corresponding SAED patterns of the samples with a pre-strain of 0 and 10%. Rodlike particles within the grains were found, and no obvious precipitates within the grain boundary were observed in both

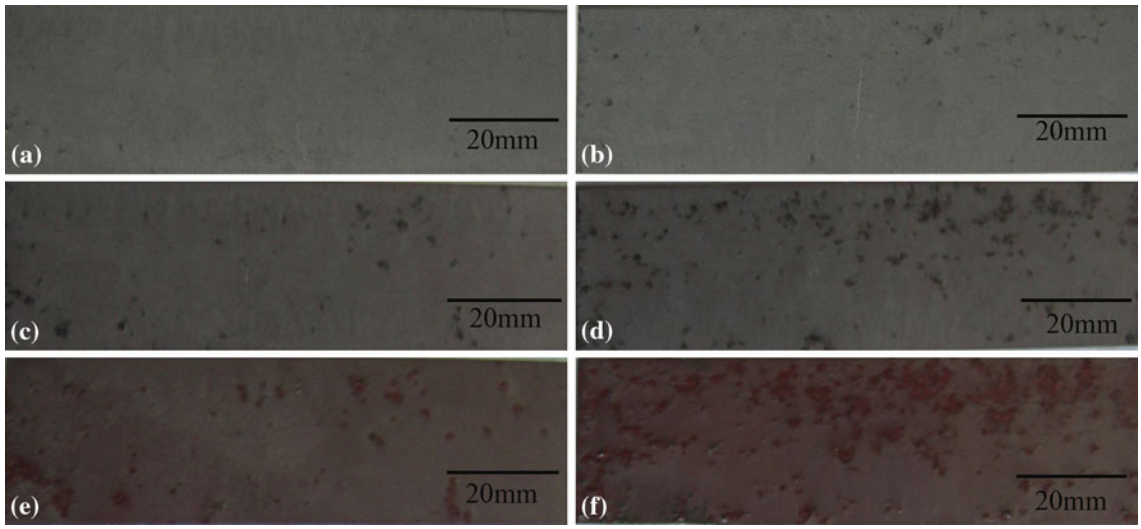

Fig. 2 Photographs of (a), (c), and (e) 0% pre-strained sample after 24, 48, and 96 h of exfoliation test, respectively; and (b), (d), and (f) 10% pre-strained sample after 24, 48, and 96 h of exfoliation test, respectively

Table 1 Results of EXCO evaluation according to ASTM G34-01 standard

Samples	6 h	12 h	24 h	48 h	72 h	96 h
0%	N	N	N	P^-	P	P^+
10%	N	N	P^-	P	P^+	EA

Table 2 Summary of corrosion parameters obtained from the polarization curves

Samples	E_{corr}, mV	I_{corr}, μA cm^{-2}
0%	−479.1	5.04
10%	−425.6	10.3

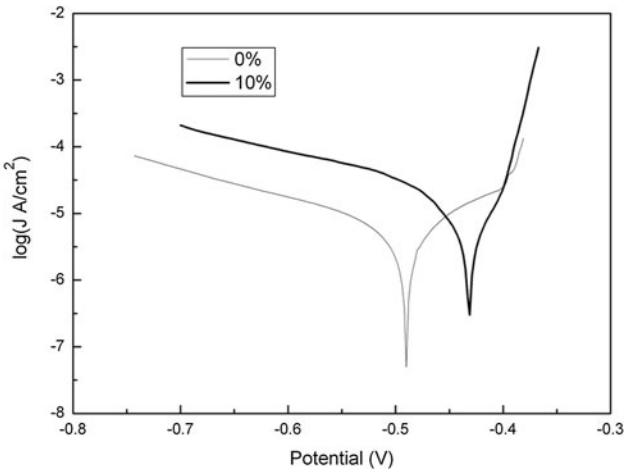

Fig. 3 Anodic potential polarization curves of Al-3.78Cu-1.67Mg alloy with a pre-strain of 0 and 10%, respectively

the samples. The rodlike particles, recognized as T phase ($Al_{20}Cu_2Mn_3$), were commonly found in Al-Cu-Mg-Mn alloys (Ref 6). According to Ref 5 and 16, streaks along $[100]_{Al}$ directions around 1/2g {220} in Fig. 5(c) and (f) demonstrated the precipitation of GPB zones in both the samples. In the 0% pre-strained sample, the density of dislocations within the grains and adjacent to the grain boundary was less. It is well known that dislocations can be generated in a metallic material during cold deformation (Ref 17), and therefore high density of dislocations was clearly visible in the 10% pre-strained sample.

3.5 Residual Stress Measurements

X-ray diffraction is one of the most advanced methods to measure residual stress of the alloy. The diffraction of x-ray is based on Bragg's law:

$$2d \sin \theta = n\lambda \quad \text{(Eq 2)}$$

where d is inter-planar spacing of two crystal attics, θ is diffraction angle, n is an integer, and λ is the wave length. The test principle of the device is a method of $2\theta_\psi$-$\sin^2 \psi$. Based on Bragg's law, the method of $2\theta_\psi$-$\sin^2 \psi$ can be described, and the residual stress of the alloy (σ) can be calculated by the following equations (Ref 18):

$$\sigma = K \times M \quad \text{(Eq 3)}$$

$$K = \frac{-E}{2(1+\nu)} \cot \theta_0 \quad \text{(Eq 4)}$$

$$M = \frac{\partial(2\theta_\psi)}{\partial \sin^2 \psi} \quad \text{(Eq 5)}$$

where K is a constant of stress measurement, M is a stress measurement factor, E is the modulus of elasticity, ν is the Poisson's ratio, and θ_0 is the diffraction angle when ψ is 0. Figure 6 shows the relationship curves between $2\theta_\psi$ and $\sin^2 \psi$. There exists an approximate linear relation between $2\theta_\psi$ and $\sin^2 \psi$, which is in agreement with Eq 4. The M and σ values of the alloy under different conditions can be obtained by linear regression in Fig. 6 and Eq 3-5. The M values of 0 and 10% pre-strained samples were 0.6613 and

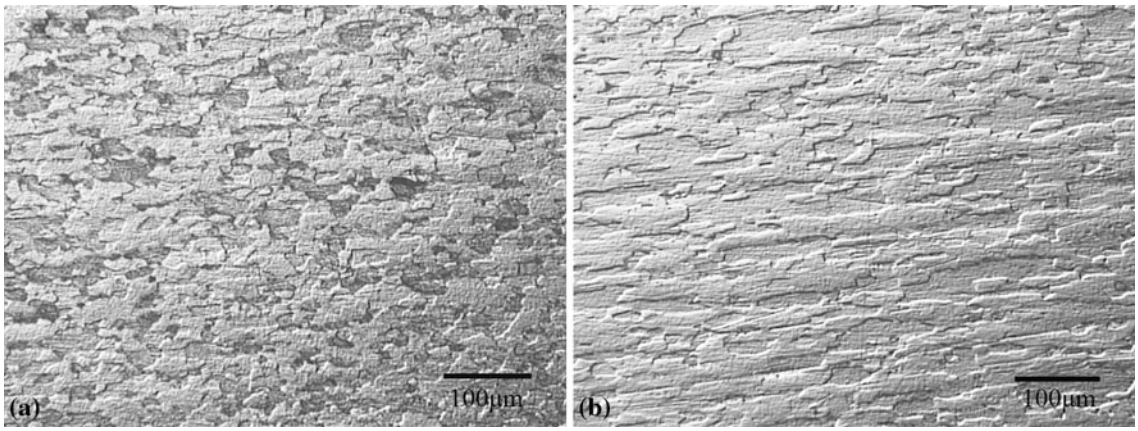

Fig. 4 Optical micrographs of cross-section of Al-3.78Cu-1.67Mg alloy for the (a) 0% pre-strained sample; (b) 10% pre-strained sample

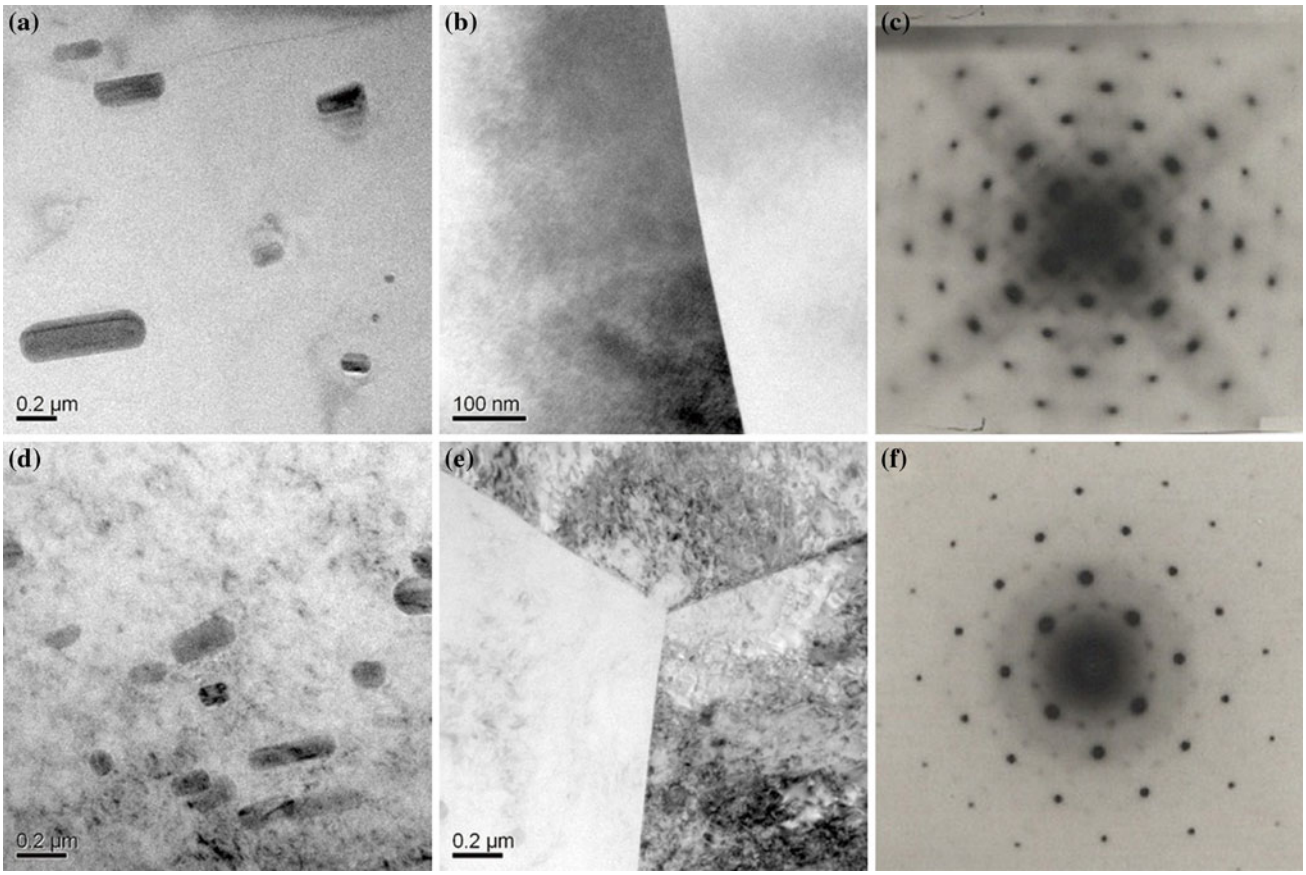

Fig. 5 TEM bright field micrographs and corresponding SAED patterns of specimens with a pre-strain of (a-c) 0%, and (d-f) 10%. The electron beam is parallel to $\langle 001 \rangle_{\alpha}$

0.4234, respectively. The residual tensile stress of the 0% pre-strained alloy was 126 MPa, while that of the alloy subjected to 10% pre-straining processing decreases to 80 MPa.

4. Discussion

The results above showed that the pre-straining processing increased the corrosion rate and corrosion current density of the alloy, and that the main differences between the nonstretched and 10% pre-strained samples were associated with some changes in the density of dislocations, grain shape, and residual tensile stress.

4.1 Effect of Dislocations Density

Anodic dissolution mechanism and hydrogen embrittlement theory were usually used to interpret the corrosion behavior of the alloy. Nevertheless, there were no obvious precipitates

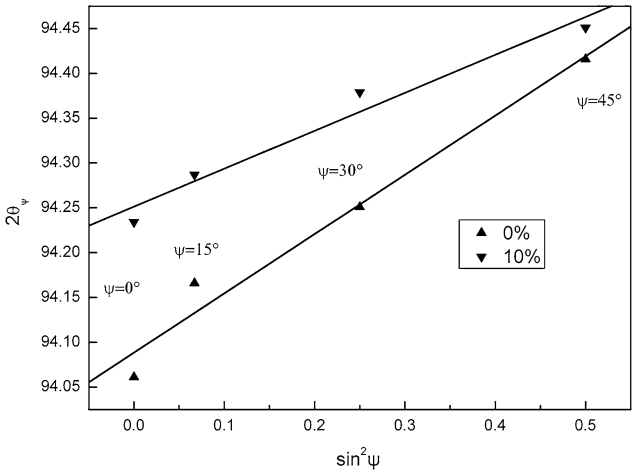

Fig. 6 Relationship between 2θ and $\sin^2 \psi$ under different conditions

within the grain boundary for both the samples; therefore, hydrogen embrittlement was the main controlling mechanism in the present study. Dislocations provide a variety of trapping sites for hydrogen to make hydrogen diffuse into the grain (Ref 19). A previous study conducted by Kamoutsi et al. (Ref 20) revealed that, hydrogen was usually produced during the corrosion process and was being trapped in distinct energy state. Albrecht et al. (Ref 21) indicated that the mobile dislocations generated in the tip of the crack would also improve the hydrogen diffusion in the matrix. Moreover, Talianker and Cina (Ref 22) investigated the stress corrosion crack (SCC) and EXCO behaviors of T651 and RRA 7000 series alloys, and demonstrated that the dislocations adjacent to the grain boundaries increased the susceptibility to SCC and EXCO of 7000 series alloys. Therefore, it was confirmed that the corrosion resistance of the alloy strongly depended on the density of dislocations.

The density of dislocations was less in the nonstretched sample, the corrosion rate was low, and only pits were detected during the EXCO test. In contrast to the nonstretched sample, the sample with a pre-strain of 10% had a higher density of dislocations within the grains and adjacent to the grain boundaries (Fig. 5), which would be expected to serve as trapping sites for the hydrogen and to enhance the solution degree of hydrogen in the alloy. This led to the occurrence of exfoliation and the accelerated growth rate of exfoliation corrosion crack. It was reasonable to infer that cold deformation before natural aging caused a pronounced increase in the density of dislocations, resulting in an increase of the susceptibility of the alloy to EXCO.

4.2 Effect of Grain Shape

The EXCO resistance of the alloy in this study is also related to the grain shape of the alloy. The corrosion products (hydrated aluminum salts and oxides) have a higher specific volume than the aluminium alloy, and the resulting expansion generates wedging force that lifts the surface grains and promote further attack. The corrosion cracks would be generated by the welding force, and then propagated along the grain boundaries (Ref 7). McNaughtan et al. (Ref 23) measured the wedging forces of high-strength aluminum alloys, and revealed that the forces were a sensitive measure of the extent of exfoliation that correlated well with the depth of attack. Lin et al. (Ref 24) investigated the effects of severe cold rolling on exfoliation corrosion behavior of Al-Zn-Mg-Cu-Cr Alloy, and found that the grain shape of the material determined the length of corrosion path and the elongated grains accelerated the growth of the corrosion cracks. More elongated grain shape produced a larger wedging stress along the grain boundary (Ref 25), thus the wedging force of the 10% pre-strained sample was higher due to the larger grain aspect ratio, resulting in a bigger stress concentration at the tip of crack and the occurrence of larger blister before fracture and spalling. This also increased the susceptibility to corrosion and corrosion rate of the alloy. Moreover, more pits were observed at the same time during the EXCO test for the 10% pre-strained sample, the number of corrosive cells enhanced greatly when remaining in electrolyte. Consequently, the sample with a pre-strain of 10% exhibits the higher corrosion current density I_{corr} value (Table 2).

4.3 Effect of Residual Tensile Stress

The results of XRD indicated that the residual tensile stress of 10% pre-strained sample was lower than that of non-stretched sample (Fig. 6). Exfoliation is a type of IGC that require a tensile component of stress at the developing corrosion tip (Ref 7). It was indicated that tensile stress lowered the breakdown potential of AA2024-T3 alloy and reduced the resistance of the alloy to corrosion (Ref 9). It is, therefore, logical to assume that the EXCO resistance of the 10% pre-strained sample would be expected to increase to some extent owing to the decrease of the residual tensile stress. However, both the immersion tests and polarization curves suggested that the pre-straining processing reduced the EXCO resistance of the alloy. Thereby the dislocations density and grain shape of the alloy are principally responsible for the EXCO resistance, and residual stress may only play a minor role in the susceptibility to EXCO.

Consequently, the pre-straining processing before natural aging tend to reduce the susceptibility to EXCO because of the decrease of residual tensile stress, which cannot totally offset the increase of the susceptibility to EXCO due to the increase of the dislocations density and grain aspect ratio, resulting in the final decrease of the EXCO resistance of the alloy.

5. Conclusion

The hardness of naturally aged Al-3.78Cu-1.67Mg alloy was significantly improved with the increasing pre-strain percents, whereas the pre-straining processing before natural aging reduced the resistance of the alloy to exfoliation corrosion. This behavior is concluded to be attributable the increase of the dislocations density and grain aspect ratio, whereas residual tensile stress may only play a minor role.

Acknowledgment

The authors would like to acknowledge the financial support of the National Key Fundamental Research Project of China.

References

1. J.C. Williams and E.A. Starke, Jr., Progress in Structural Materials for Aerospace Systems, *Acta Mater.*, 2003, **51**, p 5775–5799
2. L.S. Kramer, T.P. Blair, S.D. Blough, J.J. Fisher, Jr., and J.R. Pickens, Stress-Corrosion Cracking Susceptibility of Various Product Forms of Aluminum Alloy 2519, *J. Mater. Eng. Perform.*, 2002, **11**, p 645–650
3. Y. Li, Z. Liu, L. Lin, J. Peng, and A. Ning, Deformation Behavior of an Al-Cu-Mg-Mn-Zr Alloy During Hot Compression, *J. Mater. Sci.*, 2011, **46**, p 3708–3715
4. S.P. Ringer, K. Hono, T. Sakurai, and I.J. Polmear, Cluster Hardening in an Al-Cu-Mg Alloy, *Scripita Mater.*, 1997, **36**(5), p 517–521
5. S. Abis, M. Massazzm, P. Mengucci, and G. Riontino, Early Ageing Mechanisms in a High-Copper AlCuMg Alloy, *Scripita Mater.*, 2001, **45**, p 685–691
6. S.C. Wang and M.J. Starink, Precipitates and Intermetallic Phases in Precipitation Hardening Al-Cu-Mg-(Li) Based Alloys, *Int. Mater. Rev.*, 2005, **50**(4), p 193–215
7. M.J. Robinson and N.C. Jackson, The Influence of Grain Structure and Intergranular Corrosion Rate on Exfoliation and Stress Corrosion Cracking of High Strength Al-Cu-Mg Alloys, *Corros. Sci.*, 1999, **41**, p 1013–1028
8. J. Wloka, T. Hack, and S. Virtanen, Influence of Temper and Surface Condition on the Exfoliation Behavior of High Strength Al-Zn-Mg-Cu Alloys, *Corros. Sci.*, 2007, **49**, p 1437–1449
9. X. Liu, G.S. Frankel, B. Zoofan, and S.I. Rokhlin, Effect of Applied Tensile Stress on Intergranular Corrosion of AA2024-T3, *Corros. Sci.*, 2004, **46**, p 405–425
10. X. Liu and G.S. Frankel, Effects of Compressive Stress on Localized Corrosion in AA2024-T3, *Corros. Sci.*, 2006, **48**, p 3309–3329
11. D. Wang, D.R. Ni, and Z.Y. Ma, Effect of Pre-Strain and Two-Step Aging on Microstructure and Stress Corrosion Cracking of 7050 Alloy, *Mater. Sci. Eng. A.*, 2008, **494**, p 360–366
12. D. Yi, S. Yang, B. Deng, and M. Zhou, Effect of Pre-Strain on Fatigue Crack Growth of 2E12 Aluminum Alloy, *Trans. Nonferr. Met. Soc. China*, 2007, **17**, p 141–147
13. J. Schijce, The Effect of Pre-Strain on Fatigue Crack Growth and Crack Closure, *Eng. Fract. Mech.*, 1976, **8**, p 575–581
14. ASTM Standard G34-01, "Standard Test Method for Exfoliation Corrosion Susceptibility in 2XXX and 7XXX Series Al Alloys", 2001
15. L.D. Leshchiner, V.S. Sandler, and K.A. Sakharov, Effect of Cold Deformation on the Structure and Properties of Aluminum Alloy 1441 Sheets, *Met. Sci. Heat Treat.*, 1995, **37**, p 62–64
16. A. Charai, T. Walther, C. Alfonso, A.M. Zahra, and C.Y. Zahra, Coexistence of Clusters, GPB Zones, S″-, S′- and S-Phases in an Al ± 0.9%Cu ± 1.4%Mg Alloy, *Acta Mater.*, 2000, **48**, p 2751–2764
17. D. Wang and Z.Y. Ma, Effect of Pre-Strain on Microstructure and Stress Corrosion Cracking of Over-Aged 7050 Aluminum Alloy, *J. Alloys Compd.*, 2009, **469**, p 445–450
18. R. Gou, Y. Zhang, X. Xu, L. Sun, and Y. Yang, Residual Stress Measurement of New and In-Service X70 Pipelines by X-Ray Diffraction Method, *NDT&E Int.*, 2011, **44**, p 387–393
19. G. Itoh, K. Koyama, and M. Kanno, Evidence for the Transport of Impurity Hydrogen with Gliding Dislocation in Aluminium Alloy, *Scripta Mater.*, 1996, **35**(6), p 695–698
20. H. Kamoutsi, G.H. Haidemenopoulos, V. Bontozoglou, and S. Pantelakis, Corrosion-Induced Hydrogen Embrittlement in Aluminum Alloy 2024, *Corros. Sci.*, 2006, **48**, p 1209–1224
21. J. Albrecht, I.M. Bernstein, and A.W. Thompson, Evidence for Dislocation Transport of Hydrogen in Aluminum, *Metall. Trans. A*, 1982, **13A**, p 811–820
22. M. Talianker and B. Cina, Retrogression and Reaging and the Role of Dislocations in the Stress Corrosion of 7000-Type Aluminum Alloys, *Metall. Trans. A*, 1989, **20A**, p 2087–2092
23. D. McNaughtan, M. Worsfold, and M.J. Robinson, Corrosion Product Force Measurements in the Study of Exfoliation and Stress Corrosion Cracking in High Strength Aluminium Alloys, *Corros. Sci.*, 2003, **45**, p 2377–2389
24. L. Lin, Z. Liu, Y. Li, X. Han, and X. Chen, Effects of Severe Cold Rolling on Exfoliation Corrosion Behavior of Al-Zn-Mg-Cu-Cr Alloy, *J. Mater. Eng. Perform.*, 2011, doi:10.1007/s11665-011-9978-0
25. M.J. Robinson, Mathematical Modelling of Exfoliation Corrosion in High Strength Aluminum Alloys, *Corros. Sci.*, 1982, **22**, p 775–790